Available online at www.sciencedirect.com

ScienceDirect

Journal of Nutritional Biochemistry 89 (2021) 108573

Journal of Nutritional Biochemistry

ORIGINAL STUDY

Sulforaphane ameliorates ethanol plus carbon tetrachloride-induced liver fibrosis in mice through the Nrf2-mediated antioxidant response and acetaldehyde metabolization with inhibition of the LPS/TLR4 signaling pathway

Koji Ishida, Kosuke Kaji*, Shinya Sato, Hiroyuki Ogawa, Hirotetsu Takagi, Hiroaki Takaya, Hideto Kawaratani, Kei Moriya, Tadashi Namisaki, Takemi Akahane, Hitoshi Yoshiji

Department of Gastroenterology, Nara Medical University, Kashihara, Nara, Japan

Received 30 June 2020; received in revised form 25 November 2020; accepted 3 December 2020

Abstract

Alcoholic liver disease (ALD)-related fibrosis results from a variety of mechanisms including the accumulation of acetaldehyde, reactive oxygen species, and hepatic overload of endogenous lipopolysaccharide (LPS). Alcohol cessation is the therapeutic mainstay for patients with all stages of ALD, whereas pharmacological strategies for liver fibrosis have not been established. Sulforaphane, a phytochemical found in cruciferous vegetables, activates nuclear factor erythroid 2-related factor 2 (Nrf2) and exerts anticancer, antidiabetic, and antimicrobial effects; however, few studies investigated its efficacy in the development of ALD-related fibrosis. Herein, we investigated the effect of sulforaphane on acetaldehyde metabolism and liver fibrosis in HepaRG and LX-2 cells, human hepatoma and hepatic stellate cell lines, respectively, as well as in a mouse model of alcoholic liver fibrosis induced by ethanol plus carbon tetrachloride ($EtOH/CCl_4$). Sulforaphane treatment induced the activity of acetaldehyde-metabolizing mitochondrial aldehyde dehydrogenase in HepaRG cells and suppressed the acetaldehyde-induced proliferation and profibrogenic activity in LX-2 cells with upregulation of Nrf2-regulated antioxidant genes, including *HMOX1, NQO1,* and *GSTM3*. Moreover, sulforaphane attenuated the LPS/toll-like receptor 4-mediated sensitization to transforming growth factor-β with downregulation of NADPH oxidase 1 (*NOX1*) and *NOX4*. In $EtOH/CCl_4$-treated mice, oral sulforaphane administration augmented hepatic acetaldehyde metabolism. Additionally, sulforaphane significantly inhibited Kupffer cell infiltration and fibrosis, decreased fat accumulation and lipid peroxidation, and induced Nrf2-regulated antioxidant response genes in $EtOH/CCl_4$-treated mice. Furthermore, sulforaphane treatment blunted hepatic exposure of gut-derived LPS and suppressed hepatic toll-like receptor 4 signaling pathway. Taken together, these results suggest sulforaphane as a novel therapeutic strategy in ALD-related liver fibrosis.

Keywords: Alcoholic liver injury; Nrf2; Sulforaphane; Mitochondrial aldehyde dehydrogenase; Lipopolysaccharide; Toll-like receptor 4.

1. Introduction

Excessive alcohol consumption is associated with increased mortality worldwide due to alcoholic liver disease (ALD), a spectrum of disorders including alcoholic fatty liver disease, alcoholic hepatitis, cirrhosis, and hepatocellular carcinoma [1,2]. Currently, chronic alcohol abuse is the cause of approximately 50% of cirrhosis cases in Western countries and has become a major cause of cirrhosis in Asia [3,4]. Alcohol cessation is the mainstay of therapy for patients with all stages of ALD; however, the number of individuals succeeding in substantially abstaining from consuming alcohol is limited.

Alcoholic liver injury is commonly assumed to be caused by oxidative alcoholic metabolites including acetaldehyde-derived adducts and reactive oxygen species (ROS) predominantly produced through alcohol dehydrogenases (ADHs) and cytochrome

Abbreviations: ADH, alcohol dehydrogenase; ALD, alcoholic liver disease; ALDH, aldehyde dehydrogenase; α-SMA, alpha-smooth muscle actin; BAMBI, bone morphogenetic protein and activin membrane-bound inhibitor; CCl2, C-C motif chemokine ligand 2; CCl_4, carbon tetrachloride; CYP2E1, cytochrome P450 2E1; GAPDH, glyceraldehyde-3-phosphate dehydrogenase; GSH, glutathione; GSTM3, glutathione S-transferase 3; HMOX1, heme oxygenase 1; HSC, hepatic stellate cell; IL-1b, interleukin-1b; KC, Kupffer cell; LBP, lipopolysaccharide binding protein; LPS, lipopolysaccharide; MAA, malondialdehyde-acetaldehyde; NF-κB, nuclear factor kappa B; NOX, NADPH oxidase; NQO1, NAD (P) H: quinone oxidoreductase 1; Nrf2, nuclear factor erythroid 2-related factor 2; ROS, reactive oxygen species; TBARS, thiobarbituric acid-reactive substances; TGF, transforming growth factor; TLR, toll-like receptor; TNF, tumor necrosis factor.

* Corresponding author at: Department of Gastroenterology, Nara Medical University, 840 Shijo-cho, Kashihara, Nara 634-8521, Japan.
E-mail address: kajik@naramed-u.ac.jp (K. Kaji).

https://doi.org/10.1016/j.jnutbio.2020.108573
0955-2863/

P450 2E1 (CYP2E1), respectively, in hepatocytes [5–7]. These metabolites account for aberrant oxidative phosphorylation and mitochondrial DNA damage; lipid peroxidation products subsequently generated from accumulating oxygen free radicals and lipids also amplify oxidative damage in ALD [8,9]. Similar to other etiologies of chronic liver injury, a watershed in the development of ALD is liver fibrosis. Among the various responsible cell types, hepatic stellate cells (HSCs) play a pivotal role in ALD-related fibrogenesis. Increasing evidence demonstrate that alcohol-induced oxidative metabolites might be involved in the activation of HSCs and development of liver fibrosis [7,10]. Indeed, acetaldehyde can induce the transcription of α_1(I) and α_2(I) procollagen genes by a protein kinase C-dependent pathway and induce the secretion of transforming growth factor-β1 (TGF-β1) and the expression of TGF-β type II receptor in HSCs [11–14]. Recent studies have shown that the CYP2E1-dependent generation of ROS augments collagen I protein synthesis in cocultures of hepatocytes and HSCs [15]. Moreover, alcohol-induced production of lipopolysaccharide (LPS) in the gastrointestinal tract triggers HSC activation by increasing their susceptibility to acetaldehyde as well as TGF-β [11,16,17]. These functional mechanisms highlight the antioxidant mechanisms as a therapeutic target in ALD-related fibrosis.

Nuclear factor erythroid 2-related factor 2 (Nrf2) is a master regulator of the intracellular adaptive antioxidant response to oxidative stress [18] Under normal conditions, Nrf2 is primarily maintained in an inactivate state in the cytoplasm through binding with Kelch-like ECH-associated protein [19]. However, under conditions of oxidative stress, Nrf2 is translocated into the nucleus and binds to the antioxidant response element in the promoter regions of downstream antioxidant genes such as heme oxygenase 1 (*HMOX1*), NAD (P) H: quinone oxidoreductase 1 (*NQO1*), and glutathione (*GSH*) to induce their transcription [18,20]. Emerging evidence suggests that upregulation and transactivation of Nrf2 can delay the progression of ALD-related liver fibrosis [21,22].

Among the compounds that can activate Nrf2, sulforaphane is a dietary isothiocyanate produced by the enzymatic processing of glucoraphanin, a 4-methylsulfinylbutyl glucosinolate found in cruciferous vegetables such as broccoli and cabbage. Sulforaphane has been shown to possess antioxidative properties with multiple pharmacological actions, including anticancer, antidiabetic, and antimicrobial effects [23–25]. Remarkably, several studies have revealed the hepatoprotective effects of sulforaphane in mouse models of liver injury [26,27]. A recent study has also demonstrated that sulforaphane-mediated Nrf2 activation can induce the enzymatic activity of a mitochondrial aldehyde dehydrogenase (ALDH), ALDH2, which predominantly metabolizes acetaldehyde to nontoxic acetate in hepatocytes [28]. Moreover, sulforaphane was shown to be protective against LPS-induced, macrophage-mediated inflammation [29]. These lines of evidence highlight the promising beneficial role of sulforaphane in ALD. However, few studies have focused on whether sulforaphane efficiently alleviates the development of liver fibrosis in ALD.

In the present study, we aimed to elucidate the effects of sulforaphane on liver fibrosis induced by ethanol plus carbon tetrachloride (CCl_4) in relation to its Nrf2-mediated antioxidative and anti-inflammatory properties as well as its impact on hepatic ALDH2 activation.

2. Materials and methods

2.1. Cell culture

LX-2, a human HSC line, and HSC-T6, a rat HSC line, were purchased from Merck (Darmstadt, Germany). The human hepatoma line HepG2 was obtained from Riken BRC Cell Bank (Ibaraki, Japan). HepaRG cells were purchased from KAC Co. (Kyoto, Japan). HepaRG cells and other cell lines were cultured in RPMI-1640 medium and Dulbecco's modified Eagle medium, respectively, supplemented with 10% fetal bovine serum (Gibco, Thermo Fisher Scientific, Waltham, MA, USA) and 1% penicillin/streptomycin in an incubator at 37°C and 5% CO_2. For all assays, the cells were incubated with sulforaphane, acetaldehyde, LPS (O55:B5), and/or recombinant human TGF-β1.

Sulforaphane and acetaldehyde were purchased from Toronto Research Chemicals (Toronto, ON, Canada) and Wako Pure Chemical Industries (Osaka, Japan), respectively. LPS (O55:B5) and recombinant human TGF-β1 were obtained from Sigma-Aldrich (St. Louis, MO, USA).

2.2. Animals and experimental protocol

Ten-week-old female C57BL/6J mice (CLEA Japan, Osaka, Japan) were divided into four diet groups (n=10 mice/group). Mice in the control diet (CD) group were fed the normal liquid diet (Research Diets, New Brunswick, NJ, USA). Mice in the CD/CCl_4 group were fed the normal liquid diet and received 1 mL/kg body weight CCl_4 dissolved in corn oil (Nacalai Tesque, Kyoto, Japan) by intraperitoneal injection twice weekly. Mice in the ED/CCl_4 group were fed a 2.5% (v/v) ethanol-containing Lieber-DeCarli liquid diet (Research Diets) (ED) and received intraperitoneal CCl_4 injection twice weekly (1 mL/kg body weight) [30]. Mice in the ED/CCl_4/SFN group were fed the ED with sulforaphane and received intraperitoneal CCl_4 injection (1 mL/kg body weight) twice weekly; in this group, sulforaphane was administered peroral as a mixture of ED (5 μmoL/d/body weight) as described previously [31]. The same amount of lactose hydrate was used as vehicle for the CD, CD/CCl_4, and ED/CCl_4 groups. All mice were housed in stainless steel mesh cages under controlled conditions (23°C ± 3°C with a relative humidity of 50% ± 20%, 10–15 air changes/h, and 12 h of light/d). All animals were allowed *ad libitum* access to tap water throughout the experimental period. All mice were sacrificed after 8 weeks of feeding. At the end of the experiments, all mice underwent the following procedures: anesthesia, opening of the abdominal cavity, blood collection via aortic puncture, and harvesting of liver for histological evaluation. Serum biological markers were assessed by routine laboratory methods. Blood ethanol levels were measured by Ethanol Assay Kit (BioVision, Milpitas, CA, US) according to the manufacturer's instruction. All animal procedures were performed in compliance with the recommendations of the Guide for Care and Use of Laboratory Animals of the National Research Council, and the study was approved by the Animal Care Committee of Nara Medical University (authorization number: 12336).

2.3. ADH activity assay

ADH activity in HepaRG cells were measured by the Alcohol Dehydrogenase Assay Kit (Abcam, Cambridge, UK) according to the manufacturer's instruction.

2.4. Mitochondrial ALDH2 activity assay

ALDH2 activity in HepaRG cells and liver tissue samples were determined by the ALDH2 activity assay kit (Abcam) according to the manufacturer's protocol. ALDH2 activity was determined by measuring NADH produced as a result of the following ALDH2-catalyzed reaction: acetaldehyde + NAD^+ → acetic acid + NADH. Briefly, HepaRG cells at a concentration of 1.5×10^4 cells/mL were seeded on uncoated plastic tissue culture dishes and treated with sulforaphane at different concentrations (0–40 μM) over a time course (12–48 h). The cells as well as the homogenates from liver tissues were solubilized, and the activity solution including a reporter dye were added to the supernatants. The ALDH2 activity was determined by measuring sample absorbance at 450 nm using Multiskan FC (Thermo Fisher Scientific, Waltham, MA, USA).

2.5. Cell proliferation assay

LX-2 or HSC-T6 cells were seeded on uncoated plastic tissue culture dishes at a density of 1.5×10^4 cells/mL and treated with different concentrations of acetaldehyde (0–200 μM) and sulforaphane (0–40 μM) for 24 h. The Premix WST-1 Cell Proliferation Assay system (Takara Bio, Kusatsu, Japan) was used to assess cell proliferation.

2.6. Histological and immunohistochemical analyses

Liver specimens were fixed in 10% formalin and embedded in paraffin. For histological evaluation, 5-μm-thick sections were stained with hematoxylin/eosin and Sirius Red. For immunostaining, primary antibodies against α-smooth muscle actin (α-SMA) (ab5494, 1:200; Abcam) and F4/80 (ab100790, 1:100; Abcam) were used, according to the manufacturer's recommendations. All quantitative analyses included five fields per section at 400 × magnification and were performed by the NIH ImageJ software.

2.7. Measurement of intrahepatic thiobarbituric acid-reactive substances

After homogenization of frozen liver tissues (25 mg), intrahepatic thiobarbituric acid-reactive substances (TBARS) were assessed by measuring the hepatic content of malondialdehyde using the TBARS Assay kit (Cayman Chemical, Ann Arbor, MI, USA), according to the manufacturer's protocol.

2.8. Intrahepatic triglyceride quantification

Intrahepatic triglyceride concentrations were measured in 100 mg frozen liver tissue per animal using the Triglyceride Quantification Assay Kit (Abcam), according to the manufacturer's instructions.

2.9. Intrahepatic acetaldehyde assay

After homogenization of frozen liver tissues (40 mg), intrahepatic acetaldehyde levels were measured using the Acetaldehyde Assay kit (EACT100; BioAssay System, Hayward, CA, USA), according to the manufacturer's instructions.

2.10. RNA extraction and reverse transcription-quantitative polymerase chain reaction

Total RNA was isolated from liver tissues and cultured cells using the RNeasy Mini Kit (Qiagen, Hilden, Germany) and reverse transcribed to complementary DNA (cDNA) using the High-Capacity RNA-to-cDNA kit (Applied Biosystems, Foster City, CA, USA), according to the manufacturer's instructions. Reverse transcription-quantitative polymerase chain reaction of the cDNA with gene-specific primer pairs (**Supplementary Table. 1**) was performed using the StepOnePlus Real-time PCR system and SYBR Green from Applied Biosystems (Applied Biosystems). Relative gene expression levels were determined using glyceraldehyde-3-phosphate dehydrogenase (*GAPDH*) as the internal control. Relative target mRNA amount per cycle was determined by applying a threshold cycle to the standard curve. All reactions were performed using 1:10 diluted cDNA, and mRNA expression levels were estimated using the $2^{-\Delta\Delta CT}$ method and presented as fold changes relative to controls.

2.11. Protein extraction and western blotting

Whole-cell lysates were prepared from cultured cells. LX-2 cells (1×10^6) were preincubated with sulforaphane (5 or 20 μM) and LPS (O55:B5, 100 ng/mL) for 12 h. The T-PER tissue protein extraction reagent supplemented with proteinase and phosphatase inhibitors (Thermo Fisher Scientific) was used to prepare the lysates. The protein concentrations were measured by a Bradford protein assay (Bio-Rad, Hercules, CA, USA), and all samples were normalized to 50 μg/mL. Cellular proteins were separated by 4–12% sodium dodecyl sulfate-polyacrylamide gel electrophoresis and transferred to Invitrolon polyvinylidene difluoride membranes (Thermo Fisher Scientific). Next, the membranes were blocked with 5% bovine serum albumin in Tris-buffered saline supplemented with Tween-20 for 1 h. The following primary antibodies from Cell Signaling Technology (Danvers, MA, USA) were used for immunoblotting: ADH1 (#5295; 1:1000), ALDH2 (#18818; 1:1000), nuclear factor kappa B (NF-κB) p65 (#8242; 1:1000), phospho-NF-κB p65 (Ser536; #3033; 1:1000), and β-actin (#4967; 1:10 000). Amersham ECL horseradish peroxidase-linked IgG F(ab)2 fragment (1:5000; GE Healthcare Life Sciences, Piscataway, NJ, USA) was used as the secondary antibody. The bands were visualized using the Clarity Western ECL substrate (Bio-Rad).

2.12. Statistical analyses

Data were analyzed using Student's *t* test or one-way analysis of variance followed by Bonferroni's multiple comparison test, as appropriate. Bartlett's test was used to determine homogeneity of variances. All tests were two-tailed, and *P* values $<.05$ were considered to indicate statistical significance.

3. Results

3.1. Sulforaphane amplifies ALDH2 activity in HepaRG cells and suppresses acetaldehyde-induced proliferation and activation in LX-2 cells

We first determined whether sulforaphane could affect ADH and ALDH2 activity during ethanol and acetaldehyde metabolism in hepatocytes. As shown in Fig. 1A, HepaRG cells expressed both ADH1 and ALDH2 while HepG2 cells expressed only ALDH2. Thus, we employed HepaRG cells to evaluate the effect of sulforaphane on ethanol and acetaldehyde metabolism. In agreement with its defined role as an Nrf2 activator, sulforaphane increased the mRNA levels of Nrf2-regulated antioxidant genes including *HMOX1, NQO1,* and glutathione S-transferase 3 (*GSTM3*) in a dose-dependent manner (5, 10, 20, and 40 μM) in HepaRG cells (Fig. 1B). The ADH activity in HepaRG cells were not altered by treatment with sulforaphane at different concentrations (Fig. 1C). Meanwhile, treatment with the indicated concentrations of sulforaphane for 48 h led to significant increases in ALDH2 activity in HepaRG cells. The time-course analysis showed that the ALDH2 activity 18 h after treatment was significantly higher than that measured at the start of treatment in cells treated with 20 μM sulforaphane (Fig. 1D). We confirmed these effects of sulforaphane on ALDH2 activity in HepG2 cells (**Supplementary Fig. 1A and 1B**).

Next, we assessed the direct effect of sulforaphane on proliferative and fibrogenic activity of acetaldehyde in HSCs. As shown in Fig. 1E, acetaldehyde significantly promoted the proliferation of LX-2 cells, a human HSC line whereas treatment with sulforaphane efficiently inhibited the acetaldehyde-induced proliferation in a dose-dependent manner (Fig. 1F). Moreover, 200 μM acetaldehyde potently increased the mRNA expression levels of several markers of fibrosis, including actin alpha 2 (*ACTA2*), *TGFB1*, and *COL1A1*, whereas sulforaphane significantly lowered the observed increases in the expression levels of these genes (Fig. 1G). Additionally, we confirmed that sulforaphane exerted antiproliferative and antifibrogenic effects in HSC-T6 cells, a rat HSC line (**Supplementary Fig. 1C-1E**). We also evaluated Nrf2-mediated antioxidant response in sulforaphane-treated HSCs. In LX-2 cells, treatment with acetaldehyde did not change the mRNA levels of Nrf2-regulated antioxidant genes, the expression levels of which were significantly increased with the administration of sulforaphane (Fig. 1H). These findings suggested that sulforaphane exhibited a direct antioxidant effect via the activation of Nrf2 signaling pathways in Ac-HSCs and the induction of ALDH2 activity in hepatocytes.

3.2. Sulforaphane exerts antioxidative effects with ALDH2 induction in liver fibrosis induced by ethanol exposure in CCl_4-treated mice

Based on the observed beneficial effects of sulforaphane in hepatocytes and HSCs *in vitro*, we next assessed the effects of sulforaphane in chronic liver injury *in vivo* using ethanol in combination with CCl_4 to induce liver fibrosis in mice. The experimental protocol is shown in Fig. 2A. At the end of the experiment, the mice that received repeated administration of CCl_4 and had chronic ethanol exposure did not show significant weight loss compared to the control group (Fig. 2B). While CCl_4 administration alone did not lead to a change in liver weight, ethanol consumption significantly increased the liver weight in the CCl_4-treated mice, which was suppressed by treatment with sulforaphane (Fig. 2C). The serum levels of aspartate aminotransferase and alanine aminotransferase were elevated by CCl_4 administration, and chronic ethanol exposure augmented these changes in the CCl_4-treated mice (Fig. 2D). Interestingly, treatment with sulforaphane significantly lowered the aspartate aminotransferase and alanine aminotransferase levels in the CCl_4-treated mice exposed to ethanol (Fig. 2D). The serum albumin levels did not change by treatment with sulforaphane, suggesting that sulforaphane did not affect hepatocyte regeneration (Fig. 2E). Additionally, sulforaphane improved hypertriglyceridemia but did not alter serum cholesterol levels in the CCl_4-treated mice exposed to ethanol (Fig. 2F and 2G).

Next, we investigated hepatic ALDH2 expression and activity in our animal model. We found no difference in blood ethanol concentration between ED/CCl_4 group and ED/CCl_4/SFN group, indicating that sulforaphane did not affect ethanol absorption through gastrointestinal tract (Fig. 3A). Meanwhile, hepatic concentrations of acetaldehyde were significantly lower in mice treated with sulforaphane than those treated with vehicle in the CCl_4-treated mice exposed to ethanol suggesting that sulforaphane could efficiently promote hepatic acetaldehyde metabolism (Fig. 3B). Surprisingly, CCl_4 administration significantly downregulated the hepatic mRNA levels of *Aldh2* regardless of the ethanol exposure (Fig. 3C) whereas treatment with sulforaphane inhibited the CCl_4-mediated decrease in hepatic *Aldh2* expression (Fig. 3C). In accordance with the ob-

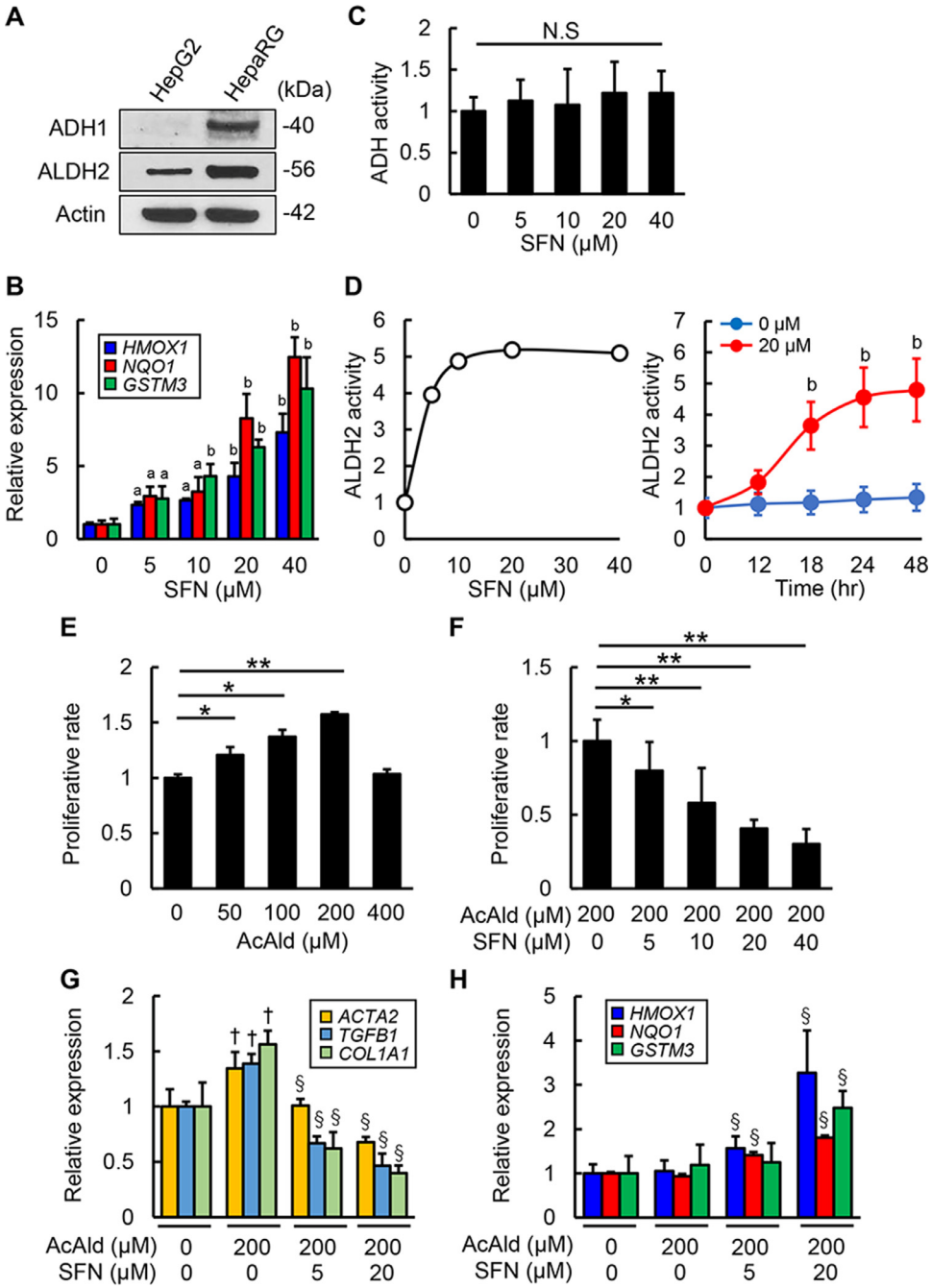

Fig. 1. Effects of sulforaphane on *in vitro* acetaldehyde metabolism and acetaldehyde-stimulated HSC activation. (A) Western blots for alcohol dehydrogenase (ADH)1 and mitochondrial aldehyde dehydrogenase (ALDH2) protein expressions in HepG2 and HepaRG cells. Actin was employed as the loading control. (B) Relative mRNA expression levels of *HMOX1, NQO1* and *GSTM3* in HepaRG cells. (C) Effect of SFN on ADH activity in HepaRG cells. (D) Dose- and time-dependent effects of SFN on ALDH2 activity in HepaRG cells. The cells were cultured for 24 h in dose-dependent assay and at 0 or 20 μM of SFN in time-dependent assay. (E) Cell proliferation of LX-2 cells stimulated by acetaldehyde (AcAld) (0, 50, 100, 200, and 400 μM). (F) Cell proliferation of LX-2 cells coincubated with 200 μM of AcAld and treated with SFN (0, 5, 10, 20, and 40 μM). (G and H) The effects of SFN on the mRNA expressions of (G) *ACTA2, TGFB1, COL1A1* and (H) *HMOX1, NQO1, GSTM3* in the AcAld-stimulated LX-2 cells. The cells were cultured with AcAld (200 μM) and SFN (0, 5, and 20 μM) for 24 h. The HepaRG cells were cultured with sulforaphane (SFN) (0, 5, 10, 20, and 40 μM) for 24 h (A-C). Quantitative values are relatively indicated as fold changes to the values of non-treatment groups. The mRNA expression levels were measured by qRT-PCR, and *GAPDH* was used as internal control for qRT-PCR. Data are mean ± SD (n=8) (A-H). $^{a}P<.05$; $^{b}P<.01$, indicating a significant difference compared with negative control (sulforaphane 0 μM) (B and D). $^{*}P<.05$; $^{**}P<.01$, indicating a significant difference between groups (C, E and F). $^{\dagger}P<.05$; $^{\S}P<.05$, indicating a significant difference compared with AcAld (0 μM)/SFN (0 μM) and AcAld (200 μM)/SFN (0 μM), respectively (G and H).

served change in *Aldh2* expression, sulforaphane prevented the loss of hepatic ALDH2 activity in the CCl_4-treated mice (Fig. 3D).

Histological evaluation with hematoxylin/eosin staining confirmed the presence of hepatic steatosis in CCl_4-treated mice exposed to ethanol and revealed that treatment with sulforaphane improved hepatic steatosis, which was confirmed by decreased levels of hepatic triglycerides (Fig. 3E and 3F). Consistent with the observed hepatic steatosis, treatment with sulforaphane significantly decreased the hepatic content of malondialdehyde, a lipid peroxidation product of polyunsaturated fatty acids, in the CCl_4-treated mice exposed to ethanol (Fig. 3G). Moreover, we found that sulforaphane upregulated the hepatic mRNA expression levels of an-

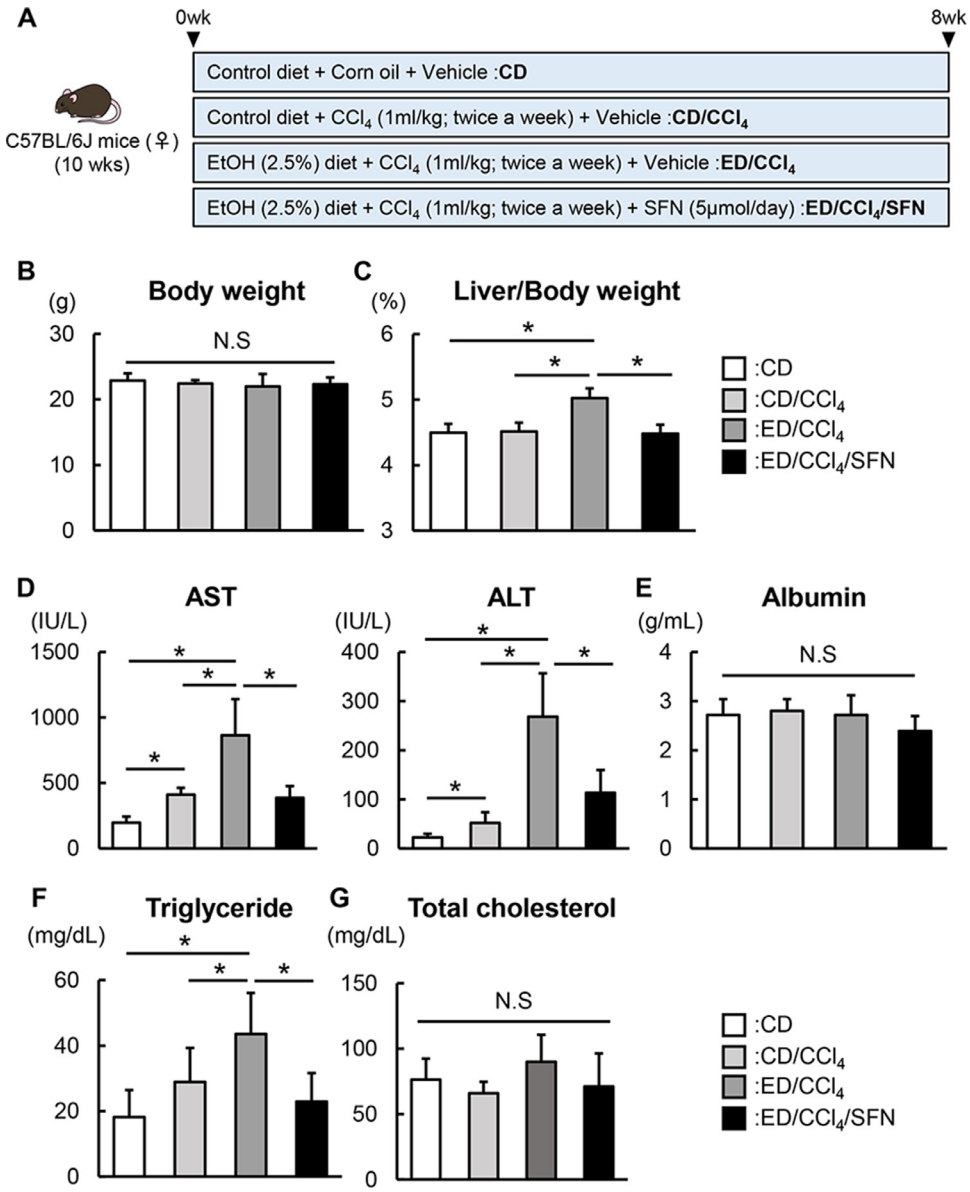

Fig. 2. Characteristic features of ethanol plus CCl_4-induced mice model. (A) Experimental protocols. (B) Body weight in the experimental groups at the end of experiment. (C) Ratio of liver weight to body weight in the experimental groups at the end of experiment. (D-G) Serum levels of aspartate transaminase (AST), alanine aminotransferase (ALT), albumin, triglyceride, and total cholesterol in the experimental groups. Data are mean ± SD (n=10). *P<.05, indicating a significant difference between groups. N.S; not significant.

tioxidant genes including *Hmox1, Nqo1,* and *Gstm3* in the CCl_4-treated mice exposed to ethanol, reflecting the augmentation of Nrf2 activation (Fig. 3H). The CCl_4-treated mice exposed to ethanol showed significantly higher mRNA levels of hepatic NADPH oxidase (*NOX*) gene family members, *Nox1, Nox2,* and *Nox4*, compared to the control mice and the mice treated with CCl_4 alone; treatment with SFN significantly reduced the observed increases in NADPH oxidase mRNA levels (Fig. 3I). These findings suggested that sulforaphane protected from oxidative stress via Nrf2 activation independently of its action on fat accumulation.

3.3. Sulforaphane protects from Kupffer cell infiltration and LPS-mediated activation of the toll-like receptor 4 signaling pathway in the liver of CCl_4-treated mice exposed to ethanol

Based on the observed improvements in ethanol- and CCl_4-induced oxidative stress following sulforaphane treatment, we next evaluated the inflammatory status in the liver specimens of mice in different experimental conditions. As shown in Fig. 4A, we observed the hepatic infiltration of F4/80-positive Kupffer cells (KCs) in the CCl_4-treated mice, which was more extensive in the CCl_4-treated mice exposed to ethanol. This expansion of KC infiltration was significantly attenuated by treatment with sulforaphane (Fig. 4A). Computer-assisted semiquantitative analysis for F4/80-positive cells revealed that the number of KCs was reduced by more than 70% with sulforaphane in the CCl_4-treated mice exposed to ethanol compared to treatment with vehicle in the CCl_4-treated mice exposed to ethanol (Fig. 4B). In parallel with the reduced infiltration of KCs, the hepatic mRNA levels of *Cd68* were significantly decreased by treatment with sulforaphane in the CCl_4-treated mice exposed to ethanol (Fig. 4C).

Next, we examined to the effect of sulforaphane on hepatic LPS/toll-like receptor 4 (TLR4) signaling pathway. The CCl_4-treated mice exposed to ethanol displayed an increase in the hepatic

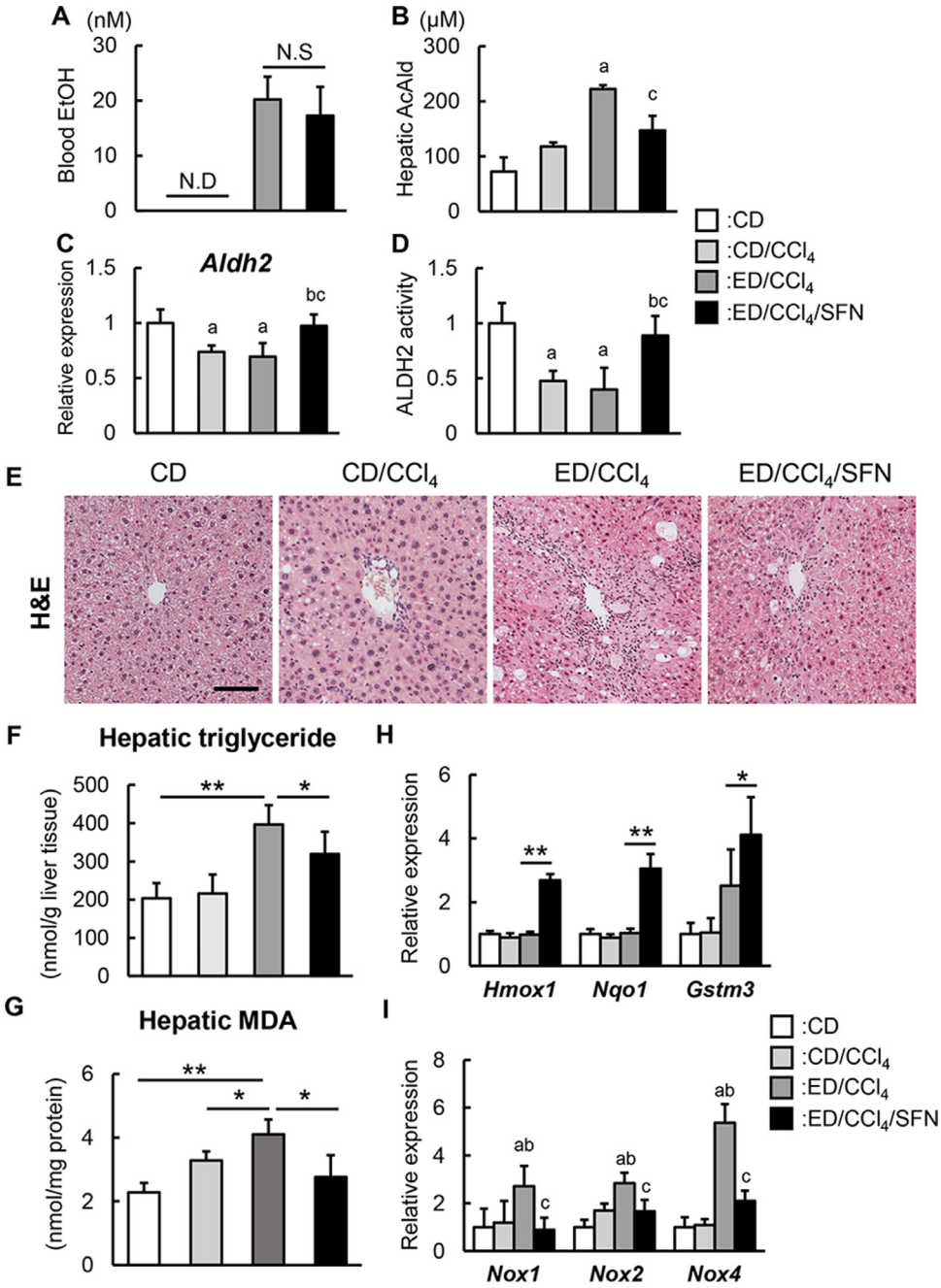

Fig. 3. Effects of sulforaphane on *in vivo* hepatic acetaldehyde metabolism, fat accumulation and oxidative stress. (A) Blood ethanol concentrations at the end of experiment. (B) Hepatic concentrations of acetaldehyde in the experimental mice. (C) Relative mRNA expression levels of *Aldh2* in the liver of experimental mice. (D) ALDH2 activity in the liver of experimental mice. Activity is indicated as fold changes to the values of CD group. (E) Representative microphotographs of hematoxylin and eosin (H&E) staining in the experimental groups. Scale bar; 50 μm. (F) Hepatic concentrations of triglyceride in the experimental groups. (G) Hepatic levels of malondialdehyde (MDA) in the experimental groups. (H and I) Relative mRNA expression levels of (H) *Hmox1, Nqo1, Gstm3* and (I) *Nox1, Nox2, Nox4* in the liver of experimental mice. Definition of experimental group is shown in Fig. 2A. The mRNA expression levels were measured by qRT-PCR, and *Gapdh* was used as internal control for qRT-PCR. Quantitative values are indicated as fold changes to the values of CD group (A, G and H). Data are mean ± SD (n=10) (A-C and E-H). $^{a}P<.05$, $^{aa}P<.01$ compared with CD group, $^{b}P<.05$, $^{bb}P<.01$ compared with CD/CCl_4 group, $^{c}P<.05$, $^{cc}P<.01$ compared with ED/CCl_4 group (A-C and E-H). N.S; not significant.

mRNA level of LPS-binding protein (*Lbp*), which binds to LPS to form a complex and interacts with the macrophage receptor to initiate a proinflammatory host response (Fig. 4D). The mRNA levels of *Tlr4* and *Cd14*, a coreceptor that functions with TLR4 to detect LPS, were upregulated in the livers of CCl_4-treated mice exposed to ethanol (Fig. 4E and 4F). Intriguingly, treatment with sulforaphane effectively abrogated the observed increases, suggesting that sulforaphane could reduce the hepatic exposure of LPS (Fig. 4D–4F). In this context, the hepatic mRNA levels of proinflammatory cytokines, including tumor necrosis factor α (*Tnfa*), interleukin 1 b (*Il1b*), and C-C motif chemokine ligand 2 (*Ccl2*), were substantially elevated in the CCl_4-treated mice exposed to ethanol whereas sulforaphane treatment led to a significant suppression of these changes observed in the CCl_4-treated mice exposed to

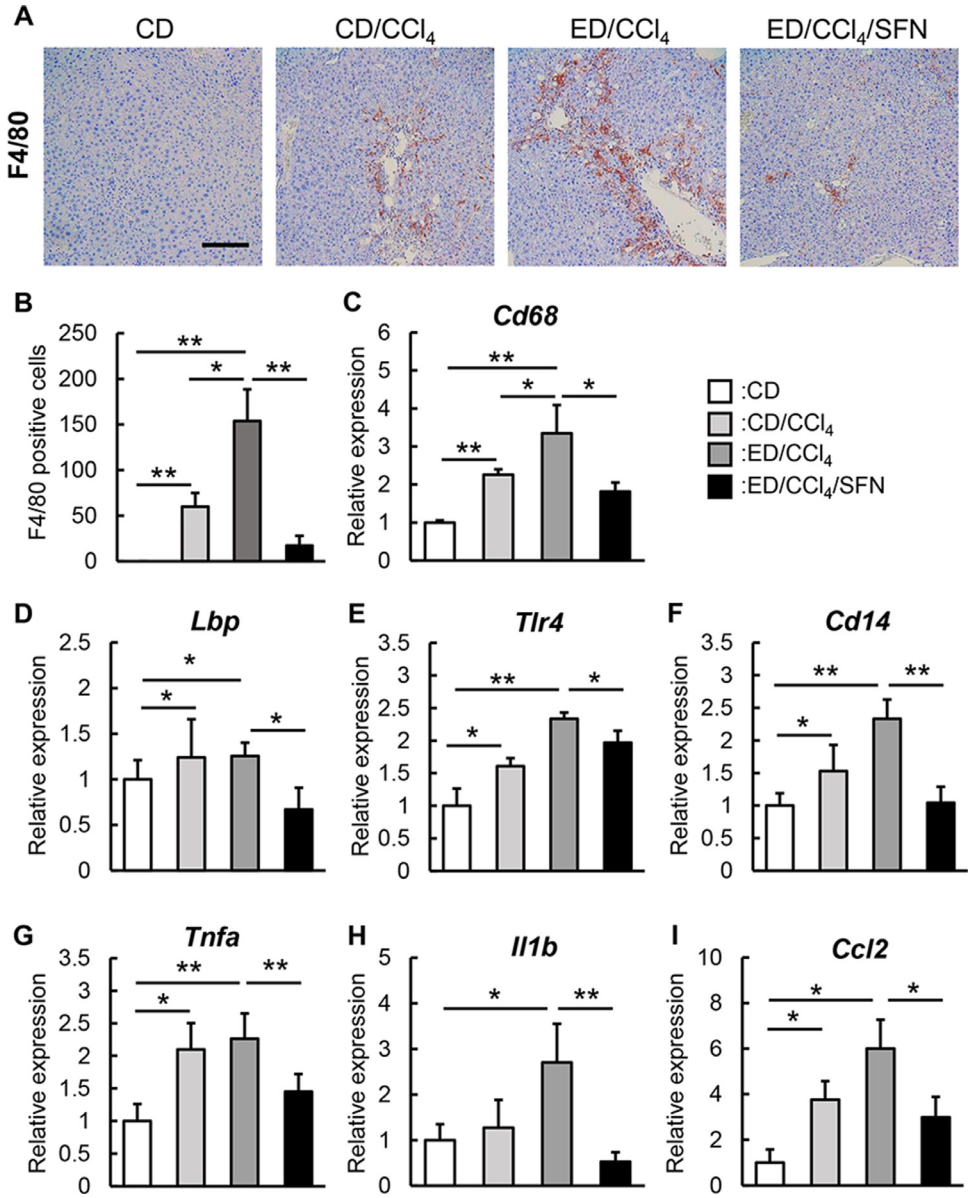

Fig. 4. Effects of sulforaphane on Kupffer cells infiltration and LPS/TLR4 signaling pathway in the ethanol plus CCl_4-induced mice. (A) Representative microphotographs of liver sections stained with F4/80. Scale bar: 50 μm. (B) Semi-quantitation of F4/80 immuno-positive Kupffer cells in high-power field (HPF) by NIH imageJ software. (C-I) Relative mRNA expression levels of (C) *Cd68*, (D) *Lbp*, (E) *Tlr4*, (F) *Cd14*, (G) *Tnfa*, (H) *Il1b*, and (I) *Ccl2* in the liver of experimental mice. The mRNA expression levels were measured by qRT-PCR, and *Gapdh* was used as internal control for qRT-PCR. Quantitative values are indicated as fold changes to the values of CD group (C-I). Data are mean ± SD (n=10), $^{*}P<.05$, $^{**}P<.01$, indicating a significant difference between groups (B-I).

ethanol (Fig. 4G–4I). These results indicated that sulforaphane alleviated hepatic inflammation via inhibition of the LPS/TLR4 signaling pathway as well as the inhibition of oxidative stress.

3.4. Sulforaphane inhibits liver fibrosis in CCl_4-treated mice exposed to ethanol

Based on the observed antioxidative and anti-inflammatory activities of sulforaphane, we assessed its effect on the development of liver fibrosis. Chronic ethanol consumption exacerbated the development of liver fibrosis in the CCl_4-treated mice, as determined by Sirius Red staining, whereas treatment with sulforaphane led to a remarkable improvement in the liver fibrosis observed in these mice (Fig. 5A). The semiquantitative analysis determined that treatment with sulforaphane led to an approximately 50% reduction in areas with fibrotic changes in the livers of CCl_4-treated mice exposed to ethanol (Fig. 5B). We also performed immunohistochemical analysis of α-SMA-stained specimens to examine the activation of HSCs, which play a pivotal role in hepatic fibrogenesis. In line with the observed attenuation of fibrosis, the α-SMA-positive areas were profoundly reduced in the sulforaphane-treated group compared with the vehicle-treated group among the CCl_4-treated mice exposed to ethanol (Fig. 5A and 5C). The observed sulforaphane-mediated suppression of hepatic fibrosis coincided with a decline in the hepatic mRNA levels of profibrotic genes including *Acta2*, *Tgfb1*, and *Col1a1* (Fig. 5D).

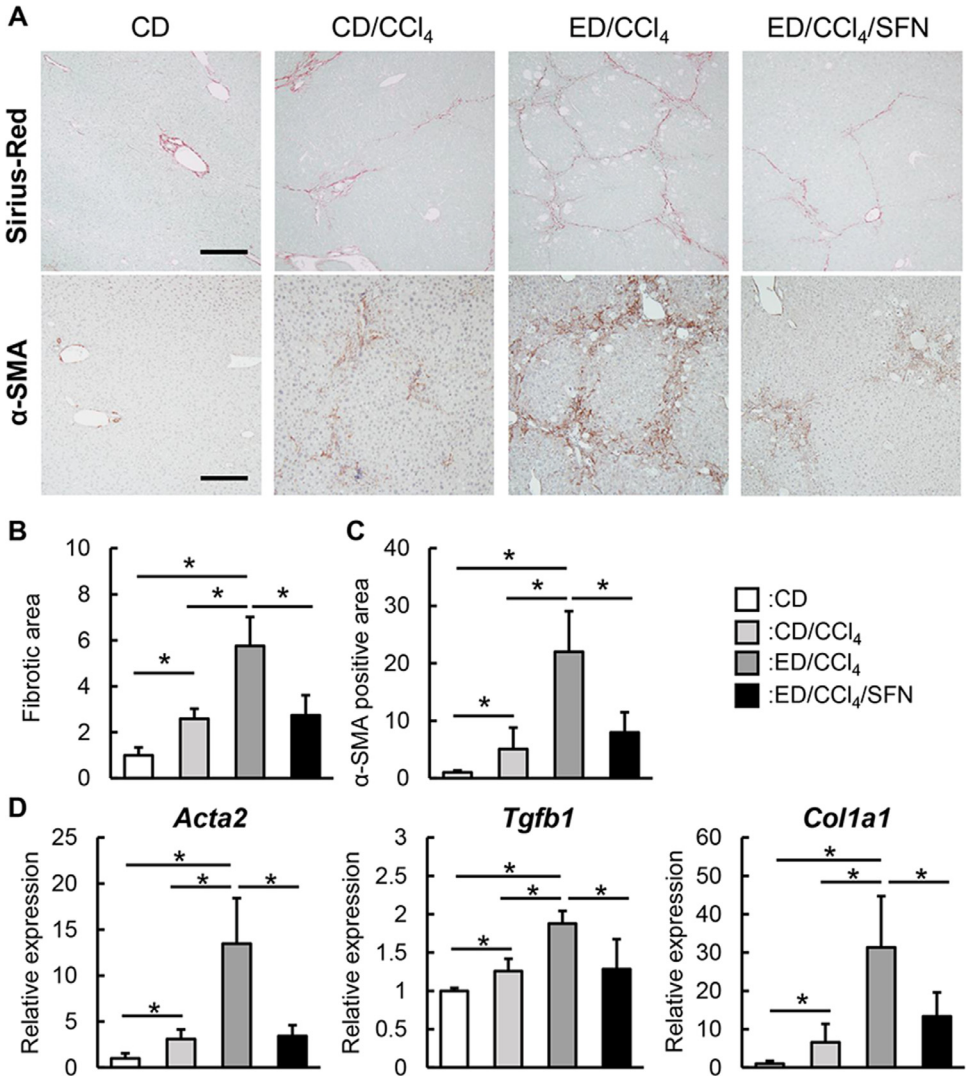

Fig. 5. Effects of sulforaphane on liver fibrosis development in the ethanol plus CCl_4-induced mice. (A) Representative microphotographs of liver sections stained with Sirius-Red and α-SMA. Scale bar; 50 μm. (B and C) Semi-quantitation of (B) Sirius-Red-stained fibrotic area and (C) α-SMA immuno-positive area in high-power field (HPF) by NIH ImageJ software. (D) Relative mRNA expression levels of *Acta2*, *Tgfb1*, and *Col1a1* in the liver of experimental mice. The mRNA expression levels were measured by qRT-PCR, and *Gapdh* was used as internal control for qRT-PCR. Quantitative values are indicated as fold changes to the values of CD group (B-D). Data are mean ± SD (n=10), $^{*}P<.05$, $^{**}P<.01$, indicating a significant difference between groups (B-D).

3.5. Sulforaphane inhibits LPS-mediated profibrogenic activity and ROS production in LX-2 cells

LPS plays a key role in the development of alcoholic liver fibrosis via activation of the TLR4/NF-κB signaling pathway in HSCs. Thus, we finally examined the impact of sulforaphane on LPS-mediated HSC activation. As shown in Fig. 6A, treatment of LX-2 cells with LPS augmented the phosphorylation of NF-κB, indicating the induction of TLR4 activation. Remarkably, treatment with sulforaphane inhibited the LPS-induced NF-κB phosphorylation (Fig. 6A). Subsequently, we assessed the impact of sulforaphane-mediated inhibition of TLR4 signaling on profibrogenic activity in LX-2 cells. In line with previous reports, LPS significantly downregulated the mRNA expression level of bone morphogenetic protein and activin membrane-bound inhibitor (*BAMBI*), a TGF-β pseudoreceptor, in LX-2 cells (Fig. 6B) [32]. Importantly, treatment with sulforaphane attenuated the LPS-mediated reduction in *BAMBI* mRNA expression in a dose-dependent manner (Fig. 6B). Furthermore, LPS augmented the TGF-β1-mediated induction of *COL1A1* and *ACTA2*, which was attenuated by treatment with sulforaphane, consistent with the increase in *BAMBI* mRNA expression (Fig. 6C). We also examined the effects of sulforaphane on the *NOX* gene family members, including *NOX1*, *NOX2*, and *NOX4*, which are relevant to oxidative stress in HSCs. Treatment with LPS induced the mRNA levels of *NOX1* and *NOX4* with no change observed in the *NOX2* mRNA levels (Fig. 6D–6F). Conversely, sulforaphane significantly reduced the upregulation of *NOX1* and *NOX4* (Fig. 6D and 6F). These results indicated that sulforaphane suppressed LPS-induced profibrogenic activity as well as NOX-derived ROS production in HSCs.

4. Discussion

In the present study, we demonstrated that the Nrf2 activator sulforaphane efficiently attenuated the progression of liver fibrosis induced by ethanol exposure in CCl_4-treated mice. We propose that the observed antifibrotic effect mediated by sulforaphane is associated with several underlying mechanisms. We first investigated the effect of sulforaphane on ALDH2 activity,

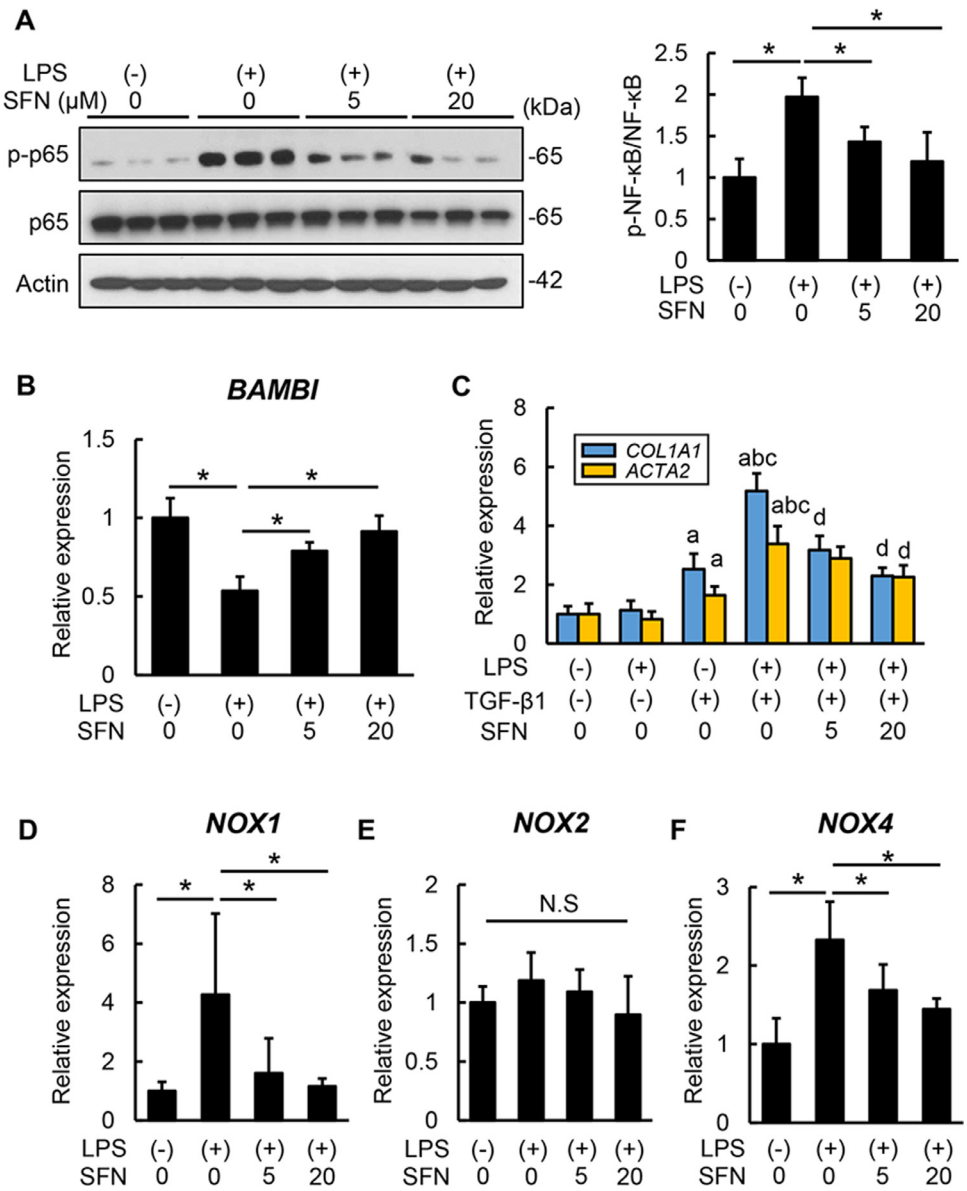

Fig. 6. Effect of sulforaphane on *in vitro* LPS-stimulated HSC activation. (A) Western blots for NF-κB p65 phosphorylation in LX-2 (left panel) and quantitative phosphorylation rate of phosphorylated NF-κB/NF-κB (right panel). Actin was used as the loading control. (B) Relative mRNA expression levels of *BAMBI* in LX-2 cells. (C) The effects of sulforaphane (SFN) on the mRNA expressions of *ACTA2* and *COL1A1* in the lipopolysaccharide (LPS) and TGF-β1-stimulated LX-2 cells. (D-F) The effects of SFN on the mRNA expressions of (D) *NOX1*, (E) *NOX2*, and (F) *NOX4* in the LPS-stimulated LX-2 cells. Cells were cultured with LPS (O55:B5, 100 ng/mL) and/or SFN (0, 5 and 20 μM) for 12 h (A), or 6 h (B and D-F), or LPS (O55:B5, 100 ng/mL) and/or recombinant human TGF-β1 (5ng/mL) and/or SFN (0, 5 and 20 μM) for 6 h (C). The mRNA expression levels were measured by qRT-PCR, and *GAPDH* was used as internal control for qRT-PCR. Quantitative phosphorylation rate is the fold changes to non-treatment groups (A-F). Data are mean ± SD (n=8), $^{*}P$<.05, indicating a significant difference between groups (A, B, and D-F). ^{a}P<.05, ^{b}P<.05, ^{c}P<.05, and ^{d}P<.05 compared with group treated with LPS(-)/TGF-β1(-)/SFN 0 μM, LPS(+)/TGF-β1(-)/SFN 0 μM, LPS(-)/TGF-β1(+)/SFN 0 μM, LPS(+)/TGF-β1(+)/SFN 0 μM, respectively (C).

which is responsible for acetaldehyde metabolism in HepaRG cells, since acetaldehyde accumulation is one of the aggravating factors in the development of ALD-related fibrosis [11]. Sulforaphane-enhanced ALDH2 activity in a dose-dependent manner in parallel with the induction of Nrf2 target genes, and time-course analysis showed that this enhancement did not occur immediately. These results suggest that sulforaphane induces ALDH2 activity indirectly via a transcriptional mechanism in HepaRG cells. Importantly, sulforaphane treatment significantly reduced hepatic acetaldehyde levels in parallel with higher ALDH2 expression and activity in mice with chronic ethanol exposure without affecting ethanol absorption through the gut. Moreover, a study recently reported that sulforaphane had a similar effect in a murine hepatoma line expressing both ALDH2 and ADH [28]. These findings strongly support our results that sulforaphane promotes acetaldehyde metabolism in liver.

We also demonstrated that sulforaphane could directly suppress the proliferation of human HSCs and acetaldehyde-mediated activation via Nrf2 transcriptional activation. Numerous studies have shown that acetaldehyde induces HSC proliferation and activation via various mechanisms [11,12,33]. On the other hand, Oh et al. have shown that sulforaphane suppresses bile duct ligation-induced liver fibrosis in mice by modulating Nrf2-mediated inhibition of the TGF-β/Smad signaling pathway in HSCs [34]. Feng et al.

have also demonstrated that sulforaphane might inhibit HSC activation through the downregulation of miR-423-5p in LX-2 cells, interfering with their activation [35]. These lines of evidence are in agreement with the present study findings and substantiate that sulforaphane contributes not only to the reduced hepatic accumulation of acetaldehyde but also to the direct protection of HSCs from acetaldehyde-induced proliferation and profibrogenic activity.

In the liver of CCl_4-treated mice exposed to ethanol, sulforaphane improved fat accumulation and reduced the levels of malondialdehyde, a marker of lipid peroxidation. Chronic ethanol-induced liver steatosis and lipid peroxidation are primarily dependent on CYP2E1, as elucidated in experiments using CYP2E1 inhibitors and *Cyp2e1* knockout and knockin mice [36–38]. Ethanol-induced steatosis was shown to be associated with the induction of CYP2E1 and increased generation of ROS and could be blocked by Nrf2-mediated antioxidant response [39,40]. In agreement with the present study results, Zhou et al. reported that sulforaphane blunted CYP2E1-dependent binge ethanol-induced liver steatosis [41]. Additionally, oral sulforaphane administration was reported to be hepatoprotective in mice with CCl_4-induced liver damage by inhibiting necrosis and ROS-induced lipid peroxidation [42]. The role of lipid peroxidation in hepatic fibrogenesis is well documented in cell and animal models, indicating that sulforaphane-mediated reduction in hepatic steatosis and hepatic malondialdehyde content contribute to the suppression of liver fibrosis induced by exposure to ethanol plus CCl_4.

The impact of hepatic macrophages, including KCs, on HSC activation is well recognized [43]. In our *in vivo* model, sulforaphane significantly decreased the number of F4/80-potitive cells and *Cd68* mRNA level as well as the mRNA levels of several proinflammatory cytokines and chemokines, namely *Tnfa*, Il1b, and *Ccl2*. These results clearly demonstrate that the anti-inflammatory effect of sulforaphane also contributes to the inhibition of liver fibrosis. Interestingly, sulforaphane exhibited a clear anti-inflammatory effect with greater magnitude than its antisteatotic effect, suggesting the involvement of additional factors in the anti-inflammatory effects of sulforaphane. We thus focused on the efficacy of sulforaphane in the context of exposure to LPS. Apparent dysbiosis is frequently observed in patients with ALD, and ethanol abuse often induces the augmentation of intestinal permeability, resulting in hepatic overload of LPS through the portal vein [44,45]. One study on a rodent cirrhotic model showed that the administration of ethanol and CCl_4 induced bacterial translocation with a marked decrease in microbial diversity [46]. Meanwhile, a recent study suggested that sulforaphane could normalize the gut microbial composition in a mouse model of bladder cancer [47]. The same study also demonstrated that sulforaphane increased the fecal levels of butyric acid and the intestinal expression levels of *Gpr41* and *Glp2*, which function to maintain the intestinal barrier function; sulforaphane also ameliorated mucosal damage by directly targeting tight junction proteins [47]. In fact, treatment with sulforaphane in our model also led to reductions in the hepatic expression levels of *Lbp, Cd14*, and *Tlr4*, markers of hepatic LPS exposure. Although these findings indicate that sulforaphane exerts an anti-inflammatory effect by potentially preventing hepatic overload of gut-derived LPS, further investigation is necessary to elucidate its effect on gut microbiota and intestinal permeability in the present model.

Moreover, we showed that sulforaphane also attenuated LPS-stimulated profibrogenic activity in HSCs. LPS-mediated activation of the TLR4/NF-κB pathway in HSCs induces the downregulation of *BAMBI*, a TGF-β pseudoreceptor, and leads to the susceptibility of HSCs to TGF-β signaling [31]. Our *in vitro* analysis showed that sulforaphane efficiently inhibited the LPS-stimulated downregulation of *BAMBI* in parallel with the suppression of TLR4/NF-κB pathway in LX-2 cells. We also found that LPS induced the upregulation of *NOX1* and *NOX4* mRNA levels, which were suppressed by sulforaphane treatment in LX-2 cells. These findings coincide with a study by Kisseleva et al. showing that both genetic and pharmacological inhibition of NOX1/NOX4 attenuated proliferative and profibrogenic activities and ROS production induced by LPS in primary mouse HSCs [48]. These results indicate the possible involvement of NOX1 and NOX4 downregulation in the inhibitory effect of sulforaphane on LPS-mediated profibrogenic activity.

The present study has several considerable limitations. First, we found that sulforaphane reduced hepatic accumulation of both malondialdehyde and acetaldehyde in ethanol exposure of CCl_4-treated mice. However, several lines of evidence have demonstrated that malondialdehyde and acetaldehyde can synergistically react with proteins and form hybrid protein conjugates referred to as malondialdehyde-acetaldehyde (MAA)-protein adducts [6]. MAA were shown to increase the secretion of chemokines involved in the chemotaxis of monocytes/macrophages and neutrophils in rat HSCs [49]. Kwon et al. have also claimed that MAA accumulation induced by the genetic deletion of *Aldh2* stimulates KCs to produce proinflammatory cytokines such as IL-6, leading to inflammation and subsequent promotion of liver fibrosis [50]. Second, the present study examined the effect of sulforaphane on ALD-related innate immunity but uncovered its effect on acquired immunity. In particular, two key mediators, IL-17, a proinflammatory chemokine, and IL-22, an anti-inflammatory cytokine, induce and repress HSC activation, respectively, in ALD-related fibrogenesis [51,52]. Thus, additional analyses are necessary to determine changes in these mediators following treatment with sulforaphane in the present model.

Collectively, our data indicate that the Nrf2 activator sulforaphane has a protective effect in the development of ALD-related fibrosis in a mouse model of liver fibrosis induced by ethanol plus CCl_4. This antifibrotic effect of sulforaphane is based on its multifaced regulatory functions including the induction of ALDH2 activity and promotion of acetaldehyde metabolism, protection of HSCs from acetaldehyde-induced profibrogenic activity, inhibition of CYP2E1-dependent lipid peroxidation, reduced hepatic LPS exposure and macrophage infiltration, and attenuated susceptibility of HSCs to TGF-β by the inhibition of TLR4 activation. As a phytochemical with limited toxicity, sulforaphane may eventually emerge as a novel treatment option for patients with ALD-related fibrosis.

Funding

This research did not receive any specific grant from funding agencies in the public, commercial, or not-for-profit sectors.

Author contribution statement

Koji Ishida: Data curation, Investigation, Formal analysis, Methodology, Writing-Original Draft Preparation. *Kosuke Kaji:* Conceptualization, Data curation, Methodology, Supervision, Validation, Visualization, Writing-Review and Editing. *Shinya Sato:* Formal analysis, Investigation, Writing-Review and Editing. *Hiroyuki Ogawa:* Investigation, Writing-Review and Editing. *Hirotetsu Takagi:* Investigation, Writing-Review and Editing. *Hiroaki Takaya:* Software, Writing-Review and Editing. *Hideto Kawaratani:* Formal analysis, Visualization, Writing-Review and Editing. *Kei Moriya:* Resources, Validation, Writing-Review and Editing. *Tadashi Namisaki:* Methodology, Writing-Review and Editing. *Takemi Akahane:* Supervision, Writing-Review and Editing. *Hitoshi Yoshiji:* Conceptualization, Supervision, Writing-Review and Editing.

Declaration of competing interest

None.

Acknowledgment

The authors would like to thank Enago (www.enago.jp) for the English language review.

Supplementary materials

Supplementary material associated with this article can be found, in the online version, at doi:10.1016/j.jnutbio.2020.108573.

References

[1] Younossi Z, Henry L. Contribution of alcoholic and nonalcoholic fatty liver disease to the burden of liver-related morbidity and mortality. Gastroenterology 2016;150:1778–85.
[2] Williams R, Alexander G, Armstrong I, Baker A, Bhala N, Camps-Walsh G, et al. Disease burden and costs from excess alcohol consumption, obesity, and viral hepatitis: fourth report of the Lancet Standing Commission on Liver Disease in the UK. Lancet. 2018;391:1097–107.
[3] Stein E, Cruz-Lemini M, Altamirano J, Ndugga N, Couper D, Abraldes JG, et al. Heavy daily alcohol intake at the population level predicts the weight of alcohol in cirrhosis burden worldwide. J Hepatol 2016;65:998–1005.
[4] Liangpunsakul S, Haber P, McCaughan GW. Alcoholic liver disease in Asia, Europe, and North America. Gastroenterology. 2016;150(8):1786–97.
[5] Lu Y, Cederbaum AI. CYP2E1 and oxidative liver Injury by alcohol. Free Radic Biol Med 2008;44:723–38.
[6] Tuma DJ, Thiele GM, Xu D, Klassen LW, Sorrell MF. Acetaldehyde and malondialdehyde react together to generate distinct protein adducts in the liver during long-term ethanol administration. Hepatology 1996;23:872–80.
[7] Gao B, Bataller R. Alcoholic liver disease: pathogenesis and new therapeutic targets. Gastroenterology 2011;141:1572–85.
[8] Lu Y, Zhuge J, Wang X, Bai J, Cederbaum AI. Cytochrome P450 2E1 contributes to ethanol-induced fatty liver in mice. Hepatology 2008;47:1483–94.
[9] Bradford BU, Kono H, Isayama F, Kosyk O, Wheeler MD, Akiyama TE, et al. Cytochrome P450 CYP2E1, but not nicotinamide adenine dinucleotide phosphate oxidase, is required for ethanol-induced oxidative DNA damage in rodent liver. Hepatology 2005;41:336–44.
[10] Paik YH, Kim J, Aoyama T, De Minicis S, Bataller R, Brenner DA. Role of NADPH oxidases in liver fibrosis. Antioxid Redox Signal 2014;20:2854–72.
[11] Chen A. Acetaldehyde stimulates the activation of latent transforming growth factor-beta1 and induces expression of the type II receptor of the cytokine in rat cultured hepatic stellate cells. Biochem J 2002;368:683–93.
[12] Svegliati-Baroni G, Ridolfi F, Di Sario A, Saccomanno S, Bendia E, Benedetti A, et al. Intracellular signaling pathways involved in acetaldehyde-induced collagen and fibronectin gene expression in human hepatic stellate cells. Hepatology 2001;33:1130–40.
[13] Greenwel P, Domínguez-Rosales JA, Mavi G, Rivas-Estilla AM, Rojkind M. Hydrogen peroxide: a link between acetaldehyde-elicited alpha1(I) collagen gene up-regulation and oxidative stress in mouse hepatic stellate cells. Hepatology 2000;31:109–16.
[14] Svegliati-Baroni G, Inagaki Y, Rincon-Sanchez AR, Else C, Saccomanno S, Benedetti A, et al. Early response of alpha2(I) collagen to acetaldehyde in human hepatic stellate cells is TGF-beta independent. Hepatology 2005;42:343–52.
[15] Nieto N, Friedman SL, Cederbaum AI. Stimulation and proliferation of primary rat hepatic stellate cells by cytochrome P450 2E1-derived reactive oxygen species. Hepatology 2002;35:62–73.
[16] Chen M, Liu J, Yang W, Ling W. Lipopolysaccharide mediates hepatic stellate cell activation by regulating autophagy and retinoic acid signaling. Autophagy 2017;13:1813–27.
[17] Seki E, De Minicis S, Osterreicher CH, Kluwe J, Osawa Y, Brenner DA, et al. TLR4 enhances TGF-beta signaling and hepatic fibrosis. Nat Med. 2007;13:1324–32.
[18] Kensler TW, Wakabayashi N, Biswal S. Cell survival responses to environmental stresses via the Keap1-Nrf2-ARE pathway. Annu Rev Pharmacol Toxicol 2007;47:89–116.
[19] Wakabayashi N, Itoh K, Wakabayashi J, Motohashi H, Noda S, Takahashi S, et al. Keap1-null mutation leads to postnatal lethality due to constitutive Nrf2 activation. Nat Genet. 2003;35:238–45.
[20] Itoh K, Wakabayashi N, Katoh Y, Ishii T, Igarashi K, Engel JD, et al. Keap1 represses nuclear activation of antioxidant responsive elements by Nrf2 through binding to the amino-terminal Neh2 Domain. Genes Dev 1999;13:76–86.
[21] Liu J, Wu KC, Lu YF, Ekuase E, Klaassen CD. Nrf2 protection against liver injury produced by various hepatotoxicants. Oxid Med Cell Longev 2013;2013:305861.
[22] Sun J, Fu J, Li L, Chen C, Wang H, Hou Y, et al. Nrf2 in alcoholic liver disease. Toxicol Appl Pharmacol 2018;357:62–9.
[23] Russo M, Spagnuolo C, Russo GL, Skalicka-Woźniak K, Daglia M, Sobarzo-Sánchez E, et al. Nrf2 targeting by sulforaphane: a potential therapy for cancer treatment. Crit Rev Food Sci Nutr 2018;58:1391–405.
[24] Axelsson AS, Tubbs E, Mecham B, Chacko S, Nenonen HA, Tang Y, et al. Sulforaphane reduces hepatic glucose production and improves glucose control in patients with type 2 diabetes. Sci Transl Med 2017;9:eaah4477.
[25] Fahey JW, Haristoy X, Dolan PM, Kensler TW, Scholtus I, Stephenson KK, et al. Sulforaphane inhibits extracellular, intracellular, and antibiotic-resistant strains of Helicobacter pylori and prevents benzo[a]pyrene-induced stomach tumors. Proc Natl Acad Sci U S A 2002;99:7610–15.
[26] Isaacson RH, Beier JI, Khoo NK, Freeman BA, Freyberg Z, Arteel GE. Olanzapine-induced liver injury in mice: aggravation by high-fat diet and protection with sulforaphane. J Nutr Biochem 2020;81:108399.
[27] Ning C, Gao X, Wang C, Huo X, Liu Z, Sun H, et al. Hepatoprotective effect of ginsenoside Rg1 from Panax ginseng on carbon tetrachloride-induced acute liver injury by activating Nrf2 signaling pathway in mice. Environ Toxicol 2018;33:1050–60.
[28] Ushida Y, Talalay P. Sulforaphane accelerates acetaldehyde metabolism by inducing aldehyde dehydrogenases: relevance to ethanol intolerance. Alcohol 2013;48:526–34.
[29] Ruhee RT, Ma S, Suzuki K. Sulforaphane protects cells against lipopolysaccharide-stimulated inflammation in murine macrophages. Antioxidants (Basel) 2019;8:577.
[30] Roychowdhury S, Chiang DJ, McMullen MR, Nagy LE. Moderate, chronic ethanol feeding exacerbates carbon-tetrachloride-induced hepatic fibrosis via hepatocyte-specific hypoxia inducible factor 1α. Pharmacol Res Perspect 2014;2:e00061.
[31] Lei P, Zhao W, Pang B, Yang X, Li BL, Ren M, et al. Broccoli sprout extract alleviates alcohol-induced oxidative stress and endoplasmic reticulum stress in C57BL/6 mice. J Agric Food Chem 2018;66:5574–80.
[32] Liu C, Chen X, Yang L, Kisseleva T, Brenner DA, Seki E. Transcriptional repression of the transforming growth factor β (TGF-β) pseudoreceptor BMP and activin membrane-bound inhibitor (BAMBI) by Nuclear Factor κB (NF-κB) p50 enhances TGF-β signaling in hepatic stellate cells. J Biol Chem 2014;289:7082–91.
[33] Chen L, Charrier AL, Leask A, French SW, Brigstock DR. Ethanol-stimulated differentiated functions of human or mouse hepatic stellate cells are mediated by connective tissue growth factor. J Hepatol 2011;55:399–406.
[34] Oh CJ, Kim JY, Min AK, Park KG, Harris RA, Kim HJ, et al. Sulforaphane attenuates hepatic fibrosis via NF-E2-related factor 2-mediated inhibition of transforming growth factor-β/Smad signaling. Free Radic Biol Med 2012;52:671–82.
[35] Feng MH, Li JW, Sun HT, He SQ, Pang J. Sulforaphane inhibits the activation of hepatic stellate cell by miRNA-423-5p targeting suppressor of fused. Hum Cell 2019;32:403–10.
[36] Cederbaum AI. Role of CYP2E1 in ethanol-induced oxidant stress, fatty liver and hepatotoxicity. Dig Dis 2010;28:802–11.
[37] Wu D, Wang X, Zhou R, Yang L, Cederbaum AI. Alcohol steatosis and cytotoxicity: the role of cytochrome P4502E1 and autophagy. Free Radic Biol Med 2012;53:1346–57.
[38] Wang Y, Kou Y, Wang X, Cederbaum A, Wang R. Multifactorial comparative proteomic study of cytochrome P450 2E1 function in chronic alcohol administration. PLoS One 2014;9:e92504.
[39] Liu J, Wang X, Peng Z, Zhang T, Wu H, Yu W, et al. The effects of insulin pre-administration in mice exposed to ethanol: alleviating hepatic oxidative injury through anti-oxidative, anti-apoptotic activities and deteriorating hepatic steatosis through SRBEP-1c activation. Int J Biol Sci 2015;11:569–86.
[40] Hsu JY, Lin HH, Hsu CC, Chen BC, Chen JH. Aqueous extract of pepino (Solanum muriactum Ait) leaves ameliorate lipid accumulation and oxidative stress in alcoholic fatty liver disease. Nutrients 2018;10:931.
[41] Zhou R, Lin J, Wu D. Sulforaphane induces Nrf2 and protects against CYP2E1-dependent binge alcohol-induced liver steatosis. Biochim Biophys Acta 2014;1840:209–18.
[42] Baek SH, Park M, Suh JH, Choi HS. Protective effects of an extract of young radish (Raphanus sativus L) cultivated with sulfur (sulfur-radish extract) and of sulforaphane on carbon tetrachloride-induced hepatotoxicity. Biosci Biotechnol Biochem 2008;72:1176–82.
[43] Nieto N. Oxidative-stress and IL-6 mediate the fibrogenic effects of [corrected] Kupffer cells on stellate cells. Hepatology 2006;44:1487–501.
[44] Szabo G. Gut-liver axis in alcoholic liver disease. Gastroenterology 2015;148:30–6.
[45] Rao R. Endotoxemia and gut barrier dysfunction in alcoholic liver disease. Hepatology 2009;50:638–44.
[46] Brenner DA, Paik YH, Schnabl B. Role of gut microbiota in liver disease. J Clin Gastroenterol 2015;49(Suppl 1):S25–7.
[47] He C, Huang L, Lei P, Liu X, Li B, Shan Y. Sulforaphane normalizes intestinal flora and enhances gut barrier in mice with BBN-Induced bladder cancer. Mol Nutr Food Res 2018;62:e1800427.
[48] Lan T, Kisseleva T, Brenner DA. Deficiency of NOX1 or NOX4 prevents liver inflammation and fibrosis in mice through inhibition of hepatic stellate cell activation. PLoS One 2015;10:e0129743.
[49] Kharbanda KK, Todero SL, Shubert KA, Sorrell MF, Tuma DJ. Malondialdehyde-acetaldehyde-protein adducts increase secretion of chemokines by rat hepatic stellate cells. Alcohol 2001;25:123–8.

[50] Kwon HJ, Won YS, Park O, Chang B, Duryee MJ, Thiele GE, et al. Aldehyde dehydrogenase 2 deficiency ameliorates alcoholic fatty liver but worsens liver inflammation and fibrosis in mice. Hepatology 2014;60:146–57.
[51] Meng F, Wang K, Aoyama T, Grivennikov SI, Paik Y, Scholten D, et al. Interleukin-17 signaling in inflammatory, Kupffer cells, and hepatic stellate cells exacerbates liver fibrosis in mice. Gastroenterology 2012;143:765–76 e3.
[52] Ma HY, Yamamoto G, Xu J, Liu X, Karin D, Kim JY, et al. IL-17 signaling in steatotic hepatocytes and macrophages promotes hepatocellular carcinoma in alcohol-related liver disease. J Hepatol 2020;72:946–59.